

Modeling the Scalar Mixing and Flavor Amplitudes

Patrick S. Walters

26 Essex Circle Drive, Shrewsbury, PA 17361

Email: patrick.walters.1980@gmail.com

March 12, 2007

Revised on November 11, 2013

Abstract

A brief discussion on the problems of light scalar meson spectroscopy is given. A mass mixing regime for pure scalar tetraquarks, pure scalar mesons, and a pure scalar glueball is presented, resulting in the realization of the experimentally observed masses in the scalar $I = 0$, $I = 1$, and $I = 1/2$ channels. The matrix elements are calculated according to $SU(3)$ flavor symmetry, OZI rules for process diagrams, and best fit to experimental data. The glueball-meson mixing elements are taken to be imaginary in order to account for the reduction in mass of the mixed glueball. The mixing matrix elements are used to compute the unitary flavor amplitude matrices, which are presented and further used to calculate theoretical partial widths for the decays $S \rightarrow P_i P_j$. New theoretical mass and error for $f_0(600)$, as well as an approximate two-pseudoscalar total width, are given in summary, along with the predicted branching ratio $\Gamma(f_{gg} \rightarrow \eta\eta)/\Gamma(f_{gg} \rightarrow \pi\pi)$ for the pure glueball state which may be present in E760 neutral data. The new states $f_0(1200 - 1600)$, $f_0(1790)$, and $X(1810)$ are mentioned as well, and explained briefly according to the new mixing scheme.

PACS numbers: 12.39.Ba, 12.39.Mk, 12.40.Yx

Introduction

One of the long-standing problems in high-energy physics is the issue of assignments for the scalar mesons. Although there is considerable controversy, at least one nonet can be justifiably established below 2 GeV. Numerous scalar signals emerge from $\pi\pi$, 4π , $\eta\eta$, $\eta\pi$, $\eta\eta'$, $K\pi$, $K\eta$, and $\bar{K}K$ final state data, enough in fact to construct two or more nonets [1]. Although one would expect to find at least one scalar nonet, a glueball, and other possible scalar objects below 2 GeV, the over-abundance of detected channels is troubling.

Currently, the Particle Data Group recognizes $f_0(1370)$, $f_0(1710)$, $a_0(1450)$, and $K_0^*(1430)$ as members of the scalar nonet [1]. However, further light scalar objects below 1 GeV may be used to organize an additional nonet of $f_0(600)$, $f_0(980)$, $a_0(980)$, and $K_0^*(800)$ [2]. There is also considerable debate as to the position of the scalar glueball. Unfortunately, data on scalar masses is still lacking, resulting in further ambiguity. With this highly troubled spectroscopy among the light scalar mesons, and different interpretations of the observed scalar channels, many authors are seeking methods to rectify the apparent crisis.

Applying the spectroscopic pattern as established in charmonium and bottomonium, one would expect to find all of the scalars in the 1.1 to 1.4 GeV range (between the 1^{--} vectors and $1^{+-}/1^{++}$ axial-vectors according to the $\mathbf{L} \cdot \mathbf{S}$ rule [2]), but instead one group is seen in the 1.3 to 1.7 GeV range and another, more controversial group in the 0.4 to 1.0 GeV range. The lighter group of scalars is often considered to be a nonet of tetraquarks or di-meson molecules. An additional well-established resonance, the $f_0(1500)$, does not appear to fit into the nearest nonet, being super-numerary. Although both observed nonets fall outside of the expected range for the nonet of “pure” scalar mesons, a mixing regime may be applied to explain this phenomenon.

Tbl. 1

Scalar state	Lighter mass (m_{γ})	Heavier mass (m_S)	Expected mass ($\mathbf{L \cdot S}$ rule)
f_0' (isosinglet)	980 ± 10	1714 ± 5	~ 1380
f_0 (isosinglet)	400 to 1200	1200 to 1500	~ 1122
a_0 (isotriplet)	984.7 ± 1.2	1474 ± 19	~ 1122
K_0^* (doublets)	$797 \pm 19 \pm 43$	1412 ± 6	~ 1168

Table 1 illustrates the problematic scalar masses from [1] with respect to the expected masses obtained by comparison to known patterns from charmonium and bottomonium spectroscopy.

Glueball-Meson Mixing Rationale

In the scalar channel, one expects the presence of 9 states in the first radial, including four traditional scalar meson groups, four scalar tetraquark groups, and one scalar glueball. The pure scalar meson masses can be obtained via the $\mathbf{L \cdot S}$ rule according to the placement of other meson states in the 1^3P band, the pure scalar tetraquark masses are easily computed from the bag model of Gottfried and Weisskopf [3], and the most accurate pure scalar glueball mass comes from the semi-unquenched lattice approximation [4]. Unfortunately, attempts to perform this mixing under the current set of theories has been unable to produce a working model, and every author appears to have their own different treatment to force correct masses out of the mixing. The results of past mixing regimes for the scalar mesons are widely varied and extremely confusing, to the point that assignments for the three heaviest scalar isosinglet states are troubled. Also, errors are large and naïvely attributed to many differing sources. Where is the real problem, and how do we fix it?

Of critical importance to understanding how to mix the scalar mesons is an understanding of how the glueball mixes with adjacent meson states to begin with. Under normal circumstances, the scalar glueball may be thought to mix with mesons and tetraquarks in the same way that tetraquarks mix with mesons, the same way that the differently flavored $I = 0$ mesons mix with each other. That is, mesons and tetraquarks mix in a mass-squared matrix with pure-state masses on the diagonal, and either positive or negative mixing mass elements outside of the diagonal. This kind of mixing, in effect, pushes the mixed masses away from one another with respect to the relative positions of

their pure-state masses, as shown in figure 1 part (a). For many years, the glueball states have been treated in the same manner as conventional mesons and tetraquarks. The results have not been truly promising or altogether agreeable. It was simply assumed that the mixing of a glueball with other mesons would follow the same pattern as meson-meson mixing, since the glueball acts like a meson and has a mass on the same order as its meson cousins. This assumption, although convenient, may not be accurate at all.

Although the glueball acts like a meson on the whole, as if it were a quark-antiquark state, it is composed of two gluons, which are entirely different in nature from quarks. Quark flavor mixing is fairly straightforward, with flavors changing via virtual boson exchanges (such as in $d \rightarrow uW^-$), heavy quark decay (such as in $s \rightarrow \bar{u}ud$), and annihilation-production reactions (such as in $\bar{d}d \rightarrow \bar{u}u$). However, gluons are not subject to any flavor changing, and are generally considered to be flavor blind. A lone gluon may be emitted by a quark, but a lone quark may not be emitted by a gluon, a difference that results from the fundamental difference between bosons and fermions. The only way gluons can mix with quarks is through the annihilation-production process $gg \rightarrow \bar{q}q$, where $q = u, d, \text{ and } s$, with probabilities $P = 1/(2 + \lambda), 1/(2 + \lambda), \text{ and } \lambda/(2 + \lambda)$ respectively, having the factor λ due to the suppression of the $\bar{s}s$ pure state formation, favoring $\bar{u}u$ - gg or $\bar{d}d$ - gg mixing over $\bar{s}s$ - gg mixing. All of these factors together, but especially the boson-boson \rightarrow fermion-fermion mixing, require a mixing scheme that causes convergence of masses, rather than divergence. This is achieved by treating the mass mixing element of the meson-glueball and tetraquark-glueball mixings as an imaginary quantity, as shown in figure 1 part (b) below;

Fig. 1

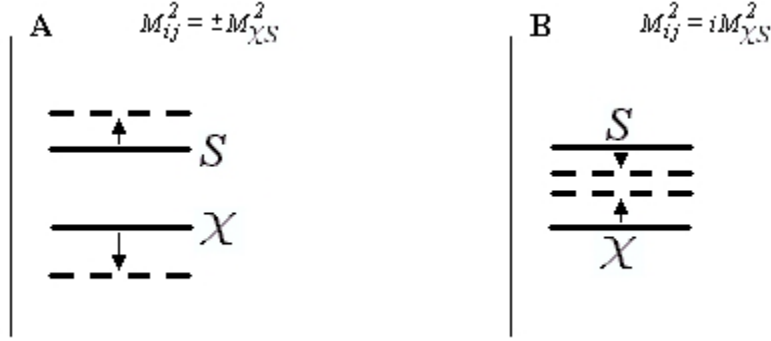


Figure 1 shows the effects of real (a) and imaginary (b) mixing mass elements. Part (a) clearly shows the mixed masses diverging as the mixing strength increases, while part (b) shows the mixed masses converging as the mixing strength increases.

This convergent behavior is a result of the difference between the strong Lagrangian for mesons composed of $\bar{\psi}_{q,a}\psi_{q,a}$ versus that for glueballs composed of $\bar{\Psi}^C\Psi^C$, as per equations 9.1 and 9.2 of [16], where the condensed field pseudo-tensor of color becomes imaginary in the Cartan sub-algebra with $[t^A, t^B] = if_{ABC}t^C$. The relative success of this treatment will be made apparent in the sections that follow.

Pure-State Masses

In order to generate mixed masses to compare with experiment, pure-state masses are calculated using the $\mathbf{L} \cdot \mathbf{S}$ rule for traditional $\bar{q}q$ mesons, and the bag model for \bar{q}^2q^2 tetraquark mesons. The $\mathbf{L} \cdot \mathbf{S}$ rule approach is straightforward, comparing the masses of all other tensor (1^3P_2) and axial-vector ($1^3P_1, 1^1P_1$) mesons and their accompanying mixing angles to find the pure-state scalar meson masses. In order to simplify the process of calculating the scalar isosinglet mixing matrix, central values omitting error bars are used, and $M_{S_q} = M_{S_a}$ is assumed. These values are $M_{S_q} = 1122$ MeV, $M_{S_s} = 1380$ MeV, $M_{S_a} = 1122$ MeV, and $M_{S_K} = 1168$ MeV for $\bar{u}u + \bar{d}d$, $\bar{s}s$, $\bar{u}u - \bar{d}d$ / $\bar{u}d$ / $\bar{d}u$, and $\bar{s}d$ / $\bar{s}u$ / $\bar{d}s$ / $\bar{u}s$ respectively.

For the tetraquarks, the three-flavor improved bag model is the only available tool for calculating the pure-state masses, as tetraquarks are not common in experiment or

well established. The bag model is much more involved than the simple $\mathbf{L} \cdot \mathbf{S}$ rule, but fortunately, the scalar tetraquarks have no orbital or spin excitations, making the bag model an ideal choice for determining mass. The tetraquark structure requires a slight adjustment of the bag model from its more traditional use with the meson. Fortunately, the generalized color-magnetic interaction formula [3];

$$R \Delta E_m = -\frac{1}{4} \alpha_s \sum_{i < j} (\lambda^i \cdot \lambda^j) (\sigma^i \cdot \sigma^j) I(\kappa_i, \kappa_j) \quad (1)$$

is capable of handling any number of quarks in a given hadron, so the tetraquark adjustment there is as easy as adding five further terms in the summation beyond the one lone term that would be necessary for a traditional meson, or three further terms beyond the three terms necessary for the traditional baryon. All of the other terms in the bag model are straightforward, and require no further alteration.

In short, the tetraquark masses are calculated by establishing a boundary condition that confines all quarks within a virtual bag, representing the confines of the tetraquark as an entity. The equation for the bag energy then becomes [3];

$$E_h = \frac{4A}{3R} \quad (2)$$

with [3];

$$A = n_q \beta_q + n_s \sqrt{\beta_s^2 + \kappa_s^2} + R \Delta E_m + R \Delta E_e \quad (3)$$

where n_q is the number of light quarks (u, d), n_s is the number of strange quarks (s), β_q and β_s are functions representing the kinetic energy of their respective quarks, and

$\kappa_s = m_s \mathbf{R}$ where m_s is taken to be the strange quark mass and \mathbf{R} is the effective bag radius. The first two terms in A describe the kinetic energy content of the constituent quarks, while the last two terms give the color-magnetic energy term from equation (1) and the color-electric energy term, which is taken to be a constant. Furthermore, the graph in figure 11 of [3] shows that β_i is a function of κ_i , roughly equal to $2.043 + (\pi - 2.043)e^{-1/\kappa}$ from its appearance. Here κ_q is taken to be zero since $m_q \approx 0$ when compared to m_s .

The actual mass of the hadron in the bag model, in this case a tetraquark, is deduced from the bag energy by the formula [3];

$$M_h = \sqrt{E_h - n_q \left(\frac{\beta_q}{R} \right)^2 - n_s \left(\frac{\beta_s}{R} \right)^2} \quad (4)$$

It should be noted that $\mathbf{R} = (A/(4\pi B))^{1/4}$ in order to reproduce the natural tendency to minimize M_h , where B is the vacuum pressure constant. In order to solve for the masses, one must first solve for κ_s since the equation for the bag radius contains terms that are κ_s -dependent. After solving for κ_s , one may proceed to solve for M_h . Fortunately, these solutions are simple enough that they may be deduced with any graphing calculator that has a solver. Solving for M_h with $B^{1/4} = 0.135$ GeV (from $M_p \approx M_n \approx 0.939$ GeV), $m_s = 0.270$ GeV (from $M_\Omega \approx 1.672$ GeV), $\alpha_s = 2.0$ (from $M_\pi \rightarrow 0$), and $\mathbf{R} \Delta E_e = 0.50$ (from all 0^+ , 1^- , $1/2^+$, and $3/2^+$ masses), the pure-state scalar tetraquark masses are as follows; $M_{\gamma q} = 854$ MeV, $M_{\gamma s} = 1372$ MeV, $M_{\gamma a} = 1372$ MeV, and $M_{\gamma K} = 1125$ MeV for $\bar{u}u \bar{d}d$, $\bar{u}u \bar{s}s + \bar{d}d \bar{s}s$, $\bar{u}u \bar{s}s - \bar{d}d \bar{s}s / \bar{u}d \bar{s}s / \bar{d}u \bar{s}s$, and $\bar{s}d \bar{u}u \pm \bar{s}d \bar{d}d / \bar{s}u \bar{u}u \pm \bar{s}u \bar{d}d / \bar{d}s \bar{u}u \pm \bar{d}s \bar{d}d / \bar{u}s \bar{u}u \pm \bar{u}s \bar{d}d$ respectively.

Last of all, a pure-state scalar glueball mass is required. For the sake of simplicity, the value is drawn from lattice calculations in another work [4]. From this selection, the pure-state glueball is considered to have a mass of $M_g = 1553$ MeV. Although all of these figures are derived from fairly simplistic and crude approaches, they certainly prove to be accurate and effective, as shown in the remainder of this work.

Pseudoscalar Flavor Amplitudes

Before one can proceed to properly obtain two-pseudoscalar S-wave decay widths from the scalar mixing, the flavor amplitudes and nature of the pseudoscalar mixing must be established. Fortunately, the experimental masses of the pseudoscalar states are well established, as are the bag model masses of η and η' [3]¹. The central experimental values, omitting errors, for the η , η' , and $\eta(1405)$ masses are $M_\eta = 547.3$ MeV, $M_{\eta'} = 957.78$ MeV, and $M_{\eta(1405)} = 1410$ MeV respectively. Thankfully, the pseudoscalar channel contains no low-lying tetraquarks, making the mixing less complicated. Assuming that $M_\eta^2 + M_{\eta'}^2 + M_{\eta(1405)}^2 = M_{Pq}^2 + M_{Ps}^2 + M_{PG}^2$, an unquenched pure-state pseudoscalar glueball mass $M_{PG} = 1639$ MeV is obtained when the bag model pseudoscalars have masses $M_{Pq} = 32$ MeV and $M_{Ps} = 720$ MeV [3]², according to the same parameters of the bag model used to find scalar tetraquark masses.

With these pure masses, one may give the pseudoscalar mesons a conventional mixing Lagrangian of the form;

$$L = -\frac{1}{2}M_{Pq}^2 P_q^2 - \frac{1}{2}M_{Ps}^2 P_s^2 + \frac{1}{2}M_G^2 G^2 - M_{PqPs}^2 P_q P_s - iM_{PqG}^2 P_q G - iM_{PsG}^2 P_s G \quad (5)$$

¹ The same overall rationale for the masses of η and η' is used here, but the quadratic mass relationship is used here, instead of the linear one, to give $M_\eta = 588$ MeV and $M_{\eta'} = 417$ MeV, as opposed to the values 530 MeV and 250 MeV respectively obtained by Gottfried and Weisskopf.

² The value for M_{Pq} is so low due to the requirement that it be near zero for small breaking of chiral symmetry. The value for M_{Ps} was taken directly from the results of Gottfried and Weisskopf, as proprietary calculations generated a slightly higher value.

Using the following 3×3 matrix;

$$M^2 = \begin{pmatrix} M_{Pq}^2 & M_{PqPs}^2 & M_{PqG}^2 \\ M_{PqPs}^2 & M_{Ps}^2 & M_{PsG}^2 \\ M_{PqG}^2 & M_{PsG}^2 & M_G^2 \end{pmatrix} \quad (6)$$

one may evaluate the mixed masses. Since the bag model mass of the η is nearly equal to its experimental mass, and must maintain its dominant $\bar{s}s$ structure, one may assume that the mixing mass M_{PsG}^2 falls close to zero since the η mass appears satisfied by the mixing M_{PqPs}^2 alone. Under this assumption, one deduces the matrix;

$$M^2 = \begin{pmatrix} M_{Pq}^2 & M_{PqPs}^2 & M_{PqG}^2 \\ M_{PqPs}^2 & M_{Ps}^2 & 0 \\ M_{PqG}^2 & 0 & M_G^2 \end{pmatrix} \quad (7)$$

Furthermore, through the determinant equation;

$$\det(M^2 - \lambda^2) = 0 \quad (8)$$

the matrix elements are evaluated, with the experimental masses being the eigenvalues λ . From this approach, one obtains $M_{PqPs}^2 = -238000 \text{ MeV}^2$ and $M_{PsG}^2 = 1181000i \text{ MeV}^2$ to fill in the matrix (with values in GeV^2);

$$M^2 = \begin{pmatrix} 0.001 & -0.238 & 1.181i \\ -0.238 & 0.518 & 0 \\ 1.181i & 0 & 2.686 \end{pmatrix} \quad (9)$$

considering that one should also mention that $M_{PdPu}^2 = 84000 \text{ MeV}^2$. Using the mixing masses to calculate the mixing angles involved, the unitary flavor amplitude matrix R for the isoscalar-pseudoscalar mesons is obtained;

$$R = \begin{pmatrix} 1.153 & 0.449 & -0.728 i \\ -0.363 & 0.932 & 0 \\ 0.679 i & 0.265 i & 1.237 \end{pmatrix} \quad (10)$$

The elements $[R_{\eta(M)I}]$ of the unitary matrix R will be useful when calculating the decay widths of scalar mesons in a later section.

Scalar Mixing Dynamics

With the pseudoscalar mixing established, one may move on to the scalar mixing. Using the pure masses established in a previous section, one again uses the conventional $I = 0$ mixing Lagrangian of the form;

$$\begin{aligned} L = & -\frac{1}{2} M_{Sq}^2 S_q^2 - \frac{1}{2} M_{\chi q}^2 \chi_q^2 + \frac{1}{2} M_G^2 G^2 - \frac{1}{2} M_{Ss}^2 S_s^2 - \frac{1}{2} M_{\chi s}^2 \chi_s^2 \\ & - M_{SqSs}^2 S_q S_s - M_{\chi q \chi s}^2 \chi_q \chi_s - i M_{SqG}^2 S_q G - i M_{\chi q G}^2 \chi_q G \\ & - i M_{SsG}^2 S_s G - i M_{\chi s G}^2 \chi_s G - M_{Sq \chi s}^2 S_q \chi_s - M_{\chi q Ss}^2 \chi_q S_s \\ & - M_{Ss \chi s}^2 S_s \chi_s - M_{Sq \chi q}^2 S_q \chi_q \end{aligned} \quad (11)$$

Additionally, one requires two more mixing Lagrangians, one for the $I = 1$ channel and one for the $I = 1/2$ channel;

$$L = -\frac{1}{2} M_{Sa}^2 S_a^2 - \frac{1}{2} M_{\chi a}^2 \chi_a^2 - M_{Sa \chi a}^2 S_a \chi_a \quad (12)$$

$$L = -\frac{1}{2} M_{SK}^2 S_K^2 - \frac{1}{2} M_{\chi K}^2 \chi_K^2 - M_{SK\chi K}^2 S_K \chi_K \quad (13)$$

Each of these requires a 2×2 mixing matrix which, for the sake of brevity and simplicity, will not be shown here. The resulting $I = 0$ 5×5 matrix, however, is as follows;

$$M^2 = \begin{pmatrix} M_{Sq}^2 & M_{SqSs}^2 & M_{SqG}^2 & M_{Sq\chi q}^2 & M_{Sq\chi s}^2 \\ M_{SqSs}^2 & M_{Ss}^2 & M_{SsG}^2 & M_{\chi qSs}^2 & M_{Ss\chi s}^2 \\ M_{SqG}^2 & M_{SsG}^2 & M_G^2 & M_{\chi qG}^2 & M_{\chi sG}^2 \\ M_{Sq\chi q}^2 & M_{\chi qSs}^2 & M_{\chi qG}^2 & M_{\chi q}^2 & M_{\chi q\chi s}^2 \\ M_{Sq\chi s}^2 & M_{Ss\chi s}^2 & M_{\chi sG}^2 & M_{\chi q\chi s}^2 & M_{\chi s}^2 \end{pmatrix} \quad (14)$$

In order to properly reduce the matrix elements, the appropriate Feynman diagrams must be accounted for. Diagrams for the processes allowed by direct transition (tree-level) appear in figure 2 below;

Fig. 2

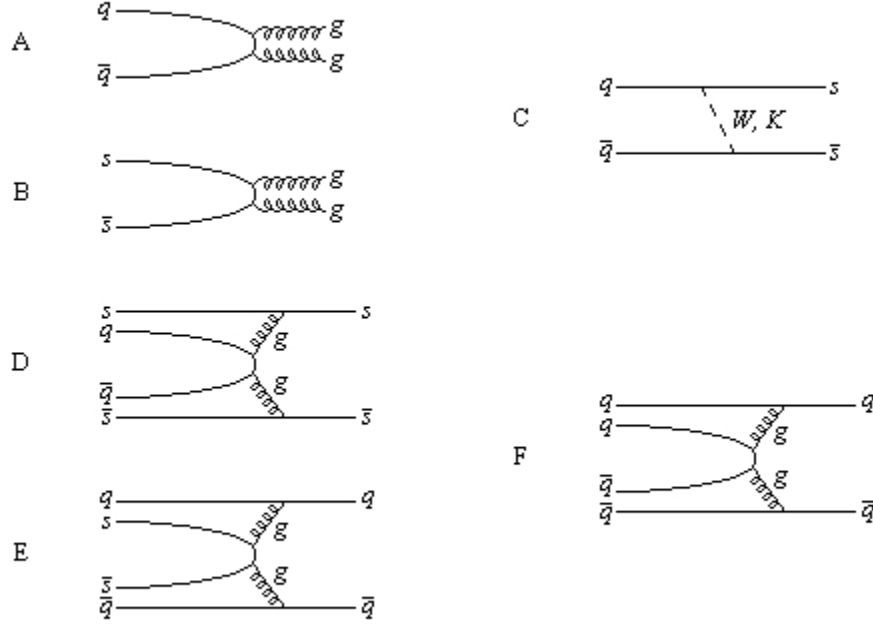


Figure 2 shows all of the viable tree-level transitions that influence the scalar mixing. Part (a) represents the transition of a light quark pair to a glueball (by annihilation), part (b) represents the transition of a strange quark pair to a glueball (by annihilation), part (c) represents the transition of a light quark pair to a strange quark pair (by virtual weak boson/kaon exchange), part (d) represents the transition of a stranded tetraquark to a strange quark pair (by annihilation and gluon exchange), part (e) represents the transition of a light tetraquark to a light quark pair (by annihilation and gluon exchange), and part (f) represents the transition of a stranded tetraquark to a light quark pair (by annihilation and gluon exchange). Note that each process is reversible. These diagrams do not include the processes where a tetraquark transitions into a glueball, since this is not diagrammatically possible as a tree-level process. Note also that the process $\bar{q}q \rightarrow \bar{s}s$ involving annihilation into gluons is not a tree-level transition either, and is OZI-violating. Taking each of these in an even-order ring/ladder approximation appears to yield self-energy induced mass.

where one finds that $M_{Ss\chi q}^2$, $M_{\chi q G}^2$, and $M_{\chi s G}^2$ must automatically reduce to zero. Other elements may be reduced by invoking flavor symmetry, allowing the reductions;

$$M_{S q \chi s}^2 \sqrt{2} = M_{S q \chi q}^2 = M_{S s \chi s}^2 \quad (15)$$

$$M_{S s G}^2 \sqrt{2} = -M_{S q G}^2 \quad (16)$$

which then give the matrix;

$$M^2 = \begin{pmatrix} M_{S q}^2 & M_{S q S s}^2 & -M_{S s G}^2 \sqrt{2} & M_{S s \chi q}^2 \sqrt{2} & M_{S s \chi q}^2 \\ M_{S q S s}^2 & M_{S s}^2 & M_{S s G}^2 & 0 & M_{S s \chi q}^2 \sqrt{2} \\ -M_{S s G}^2 \sqrt{2} & M_{S s G}^2 & M_G^2 & 0 & 0 \\ M_{S s \chi q}^2 \sqrt{2} & 0 & 0 & M_{\chi q}^2 & M_{\chi q \chi s}^2 \\ M_{S s \chi q}^2 & M_{S s \chi q}^2 \sqrt{2} & 0 & M_{\chi q \chi s}^2 & M_{\chi s}^2 \end{pmatrix} \quad (17)$$

Using the target masses $M_{f_0(980)} = 980$ MeV, $M_{f_0(1370)} = 1350$ MeV, $M_{f_0(1500)} = 1507$ MeV, and $M_{f_0(1710)} = 1714$ MeV from experiment [1] excluding errors, one finds, first of all, that $M_{f_0(600)} = 441$ MeV (which matches the prediction of [5]) since $M_{S q}^2 + M_{\chi q}^2 + M_G^2 + M_{S s}^2 + M_{\chi s}^2 = M_{f_0(600)}^2 + M_{f_0(980)}^2 + M_{f_0(1370)}^2 + M_{f_0(1500)}^2 + M_{f_0(1710)}^2$. Secondly, the matrix elements may be deduced and exact masses for the mixed states found by solving the matrix based on the most well known experimental masses (since others are not well established). The result of much tedious calculation gives $M_{\chi q \chi s}^2 = 420000 \pm 40000$ MeV², $M_{S s G}^2 = -190000i \pm 10000i$ MeV², $M_{S q \chi s}^2 = 520000 \pm 10000$ MeV², $M_{S q S s}^2 = 210000 \pm 20000$ MeV², and the matrix (with values in GeV²);

$$M^2 = \begin{pmatrix} 1.259 & 0.210 & 0.269i & 0.735 & 0.520 \\ 0.210 & 1.904 & -0.190i & 0 & 0.735 \\ 0.269i & -0.190i & 2.412 & 0 & 0 \\ 0.735 & 0 & 0 & 0.729 & 0.420 \\ 0.520 & 0.735 & 0 & 0.420 & 1.882 \end{pmatrix} \quad (18)$$

Additionally, the mixing masses $M_{S\eta\chi}^2 = -520000 \pm 10000 \text{ MeV}^2$, $M_{\gamma d\eta u}^2 = -10000 \pm 10000 \text{ MeV}^2$, and $M_{SdSu}^2 = -5000 \pm 5000 \text{ MeV}^2$ can be combined with the $I = 0$ matrix; the first mixing mass is specific to the $I = 1$ channel, while the second and third mixing masses are for the $\bar{d}d \bar{s}s \rightarrow \bar{u}u \bar{s}s$ and $\bar{d}d \rightarrow \bar{u}u$ mixings respectively, which produce the $I = 0$ and $I = 1$ channels. Using the errors in the $I = 0$ 5×5 matrix elements (fixed by the $f_0(1500)$ and $f_0(1710)$ mass errors from experiment), the mixed masses from the matrix (18) become $M_{f_0(600)} = 457 \pm 13 \text{ MeV}$, $M_{f_0(980)} = 979 \pm 6 \text{ MeV}$, $M_{f_0(1370)} = 1342 \pm 7 \text{ MeV}$, $M_{f_0(1500)} = 1505 \pm 7 \text{ MeV}$, and $M_{f_0(1710)} = 1717 \pm 7 \text{ MeV}$, as compared to the experimental values $M_{f_0(600)} = 400 \text{ to } 1200 \text{ MeV}$, $M_{f_0(980)} = 980 \pm 10 \text{ MeV}$, $M_{f_0(1370)} = 1200 \text{ to } 1500 \text{ MeV}$, $M_{f_0(1500)} = 1507 \pm 5 \text{ MeV}$, and $M_{f_0(1710)} = 1714 \pm 5 \text{ MeV}$ [1]. Indeed, the mass $M_{f_0(600)}$ falls closely in line with the prediction of [5], and all other masses are acceptably within experimental limits. Additionally, the masses $M_{a_0(980)} = 985 \pm 6 \text{ MeV}$ and $M_{a_0(1450)} = 1475 \pm 3 \text{ MeV}$ emerge when $M_{S\eta\chi}^2$ in the $I = 1$ channel is identical in magnitude and opposite in sign to $M_{S\eta\eta}^2$ in the $I = 0$ channel (compare to $M_{a_0(980)} = 984.7 \pm 1.2 \text{ MeV}$ and $M_{a_0(1450)} = 1474 \pm 19 \text{ MeV}$ from [1]), and the masses $M_{K^*0(800)} = 797 \pm 11 \text{ MeV}$ and $M_{K^*0(1430)} = 1412 \pm 7 \text{ MeV}$ emerge with $M_{SK\chi K}^2 = 678000 \pm 18000 \text{ MeV}^2$ (compare to $M_{K^*0(800)} = 797 \pm 43 \pm 19 \text{ MeV}$ and $M_{K^*0(1430)} = 1412 \pm 6 \text{ MeV}$ from [1]).

Tbl. 2

Scalar state	Light scalar mass (m_{γ})	Standard mass (m_S)	Mixing mass
f_0' (isosinglet)	979 ± 6	1717 ± 6	858 ± 9
f_0 (isosinglet)	457 ± 13	1342 ± 7	858 ± 9
a_0 (isotriplet)	985 ± 6	1475 ± 3	721 ± 7
K_0^* (doublets)	797 ± 11	1412 ± 7	823 ± 11

Table 2 shows the mass values deduced from the scalar mixing matrices, and the mixing mass from the meson-tetraquark mixing in each set.

The scalar mixing angles are deduced from the mixing elements, and converted into a unitary flavor amplitude matrix, much the same as was done for the pseudoscalars in the previous section. The unitary 5×5 matrix is as follows;

$$R = \begin{pmatrix} 0.701 & -0.208 & -0.171i & -0.500 & -0.492 \\ -0.127 & 0.841 & 0.369i & 0.199 & -0.611 \\ 0.132i & -0.468i & 1.112 & 0 & 0 \\ 0.404 & -0.365 & -0.202i & 0.840 & -0.192 \\ 0.588 & 0.578 & 0.174i & 0.062 & 0.590 \end{pmatrix} \quad (19)$$

The masses of the scalar mesons, shown in their full mixing in figure 3, and the newly found flavor amplitudes $[R_{\gamma_0(M)_I}]$ are a prediction of this work, as well as the S-wave two-pseudoscalar decay widths that will follow from these parameters in the next section.

Fig. 3

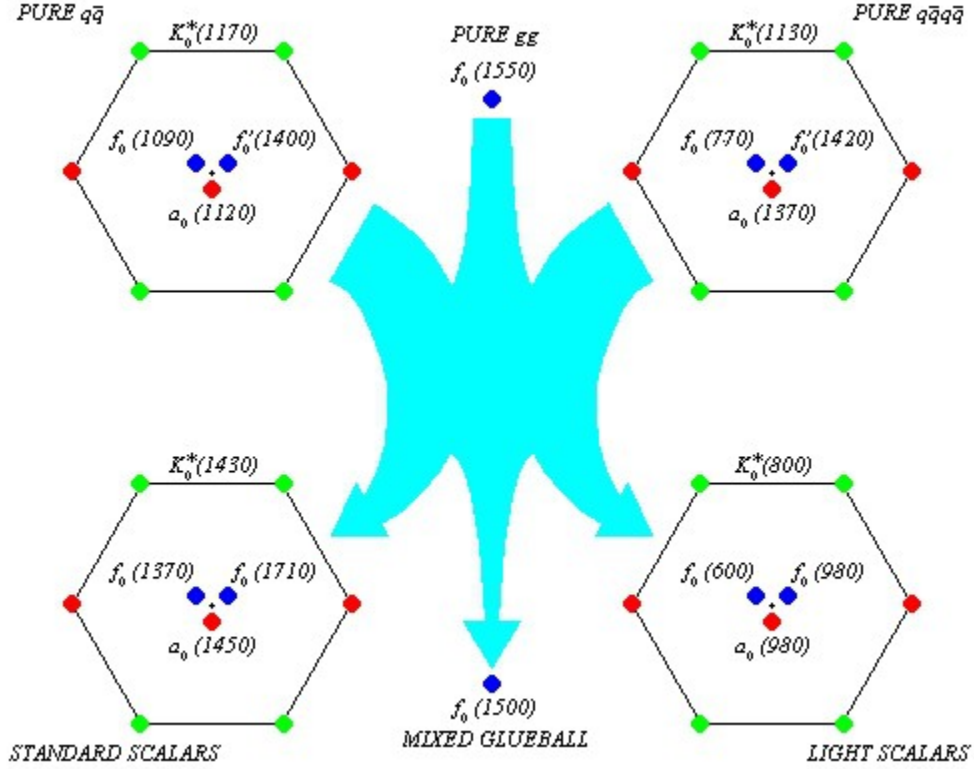


Figure 3 is an illustration of the pure scalar meson nonet (upper left, with internal $I = 0$ and isoscalar-isovector mixings enforced), the pure scalar tetraquark nonet (upper right, with internal $I = 0$ and isoscalar-isovector mixings enforced), standard scalar nonet (lower left), and light scalar nonet (lower right). The pure scalar glueball is at the top and center, while the mixed scalar glueball is at the bottom and center.

Decays of Scalar Mesons

The scalar meson states found in the previous section are capable of decaying in S-wave into two pseudoscalar mesons, whose combined isospin are appropriate to the isospin channel of each scalar. The scalars are also capable of decaying into two vector mesons in S-wave, but the dynamics of that situation require further work before they can be presented. In short, figure 4 below illustrates the most general $S \rightarrow P_i P_j$ decay diagrams used to generate couplings for the width calculations to follow.

Fig. 4

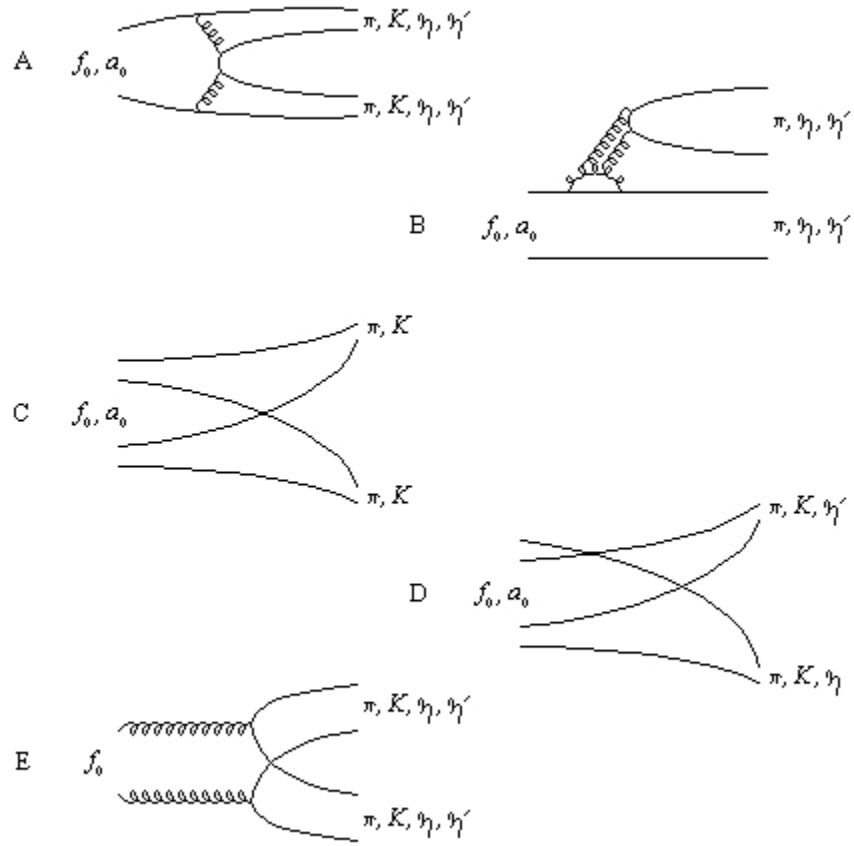


Figure 4 shows all of the viable tree-level decay processes for the $I = 0, 1$ scalar mesons. The $I = 1/2$ scalar mesons are not shown here, but have similar processes by extension. Part (a) is the conventional mechanism for scalar meson decay, while part (b) is a penguin-diagram decay similar in results to the first. Parts (c) and (d) are the so-called “fall apart” mechanism for tetraquark decay, and part (e) is a gluon-fission decay. These Feynman diagrams are the driving framework behind the reduced partial widths of equation (20) which follow.

From the previously solved flavor amplitude matrices, the scalar decays into two pseudoscalar mesons follow according to extensions to the generalized partial width equations in table 14.4 of [1] and, by extension, table 1 of [6] as follows;

$$\begin{aligned}
\gamma^2_{f_0 \rightarrow \pi\pi} &= 3 ((R_{\pi q}^2 + R_{\pi a}^2) R_{Sq} + R_{\pi s}^2 R_{Ss} \sqrt{2} + r_2 R_G + (R_{\pi q} \sqrt{2} - R_{\pi s})^2 r_3 R_G \\
&\quad + i R_{\pi G}^2 R_G + x_q (R_{\pi q}^2 + R_{\pi a}^2) R_{\chi q} \sqrt{2} + x_s R_{\pi q} R_{\pi s} R_{\chi s})^2 \\
\gamma^2_{f_0 \rightarrow \eta\eta} &= ((R_{\eta q}^2 + R_{\eta a}^2) R_{Sq} + R_{\eta s}^2 R_{Ss} \sqrt{2} + r_2 R_G + (R_{\eta q} \sqrt{2} - R_{\eta s})^2 r_3 R_G \\
&\quad + i R_{\eta G}^2 R_G + x_q (R_{\eta q}^2 + R_{\eta a}^2) R_{\chi q} \sqrt{2} + x_s R_{\eta q} R_{\eta s} R_{\chi s})^2 \\
\gamma^2_{f_0, a_0 \rightarrow \bar{K}K} &= (R_{Sq} + R_{Ss} \sqrt{2} + 2r_2 R_G + x_s R_{\chi s})^2 + (R_{Sa} + x_s R_{\chi a})^2 \\
\gamma^2_{f_0 \rightarrow \eta\eta'} &= 2 ((R_{\eta q} R_{\eta' q} + R_{\eta a} R_{\eta' a}) R_{Sq} + R_{\eta s} R_{\eta' s} R_{Ss} \sqrt{2} \\
&\quad + (R_{\eta' q} \sqrt{2} - R_{\eta' s}) (R_{\eta q} \sqrt{2} - R_{\eta s}) r_3 R_G + i R_{\eta G} R_{\eta' G} R_G \\
&\quad + x_q (R_{\eta q} R_{\eta' q} + R_{\eta a} R_{\eta' a}) R_{\chi q} \sqrt{2} + x_s (R_{\eta q} R_{\eta' s} + R_{\eta s} R_{\eta' q}) R_{\chi s})^2 \\
\gamma^2_{a_0 \rightarrow \eta\pi} &= 2 ((R_{\eta q} R_{\pi a} + R_{\eta a} R_{\pi q}) R_{Sa} + x_s (R_{\eta a} R_{\pi s} + R_{\eta s} R_{\pi a}) R_{\chi a})^2 \\
\gamma^2_{a_0 \rightarrow \eta'\pi} &= 2 ((R_{\pi q} R_{\eta' a} + R_{\pi a} R_{\eta' q}) R_{Sa} + x_s (R_{\pi a} R_{\eta' s} + R_{\pi s} R_{\eta' a}) R_{\chi a})^2 \\
\gamma^2_{K^*0 \rightarrow K\pi} &= ((R_{SK} - x_K R_{\chi K}) (R_{\pi q} + R_{\pi s} / \sqrt{2}))^2 + ((R_{SK} - x_K R_{\chi K}) R_{\pi a})^2 \\
\gamma^2_{K^*0 \rightarrow K\eta} &= ((R_{SK} - x_K R_{\chi K}) (R_{\eta q} + R_{\eta s} / \sqrt{2}))^2 + ((R_{SK} - x_K R_{\chi K}) R_{\eta a})^2
\end{aligned} \tag{20}$$

To convert these reduced partial widths into partial widths extended from equation (14.18) in [1], we take the formulae;

$$\begin{aligned}
\Gamma_{f_0 \rightarrow P_1 P_2} &= 4C (9R_G^2/4 + (1 - R_G^2)) \gamma^2_{f_0 \rightarrow P_1 P_2} |F(q)|^2 q \\
\Gamma_{a_0 \rightarrow P_1 P_2} &= 4C (9R_G^2/4 + (1 - R_G^2)) \gamma^2_{a_0 \rightarrow P_1 P_2} |F(q)|^2 q \\
\Gamma_{K^*0 \rightarrow P_1 P_2} &= 4C \gamma^2_{K^*0 \rightarrow P_1 P_2} |F(q)|^2 q
\end{aligned} \tag{21}$$

with the S-wave form factor from [1];

$$|F(q)|^2 = e^{-t}, t = q^2/(8\beta^2) \quad (22)$$

where $C = 0.004$ is a nonet constant from a best fit to data, the factor 4 is due to the multiplicity factor $(2S_1 + 1)(2S_2 + 1)/(2J + 1)$ where $J = 0$ and $S_1 = S_2 = 1/2$, $q = \sqrt{(M_S^2 - (M_{P_i} + M_{P_j})^2)/2}$ is the momentum of each of pseudoscalars in the center-of-mass of the decaying scalar, and $\beta \approx 500$ MeV is a scale factor. Merging equations (20), (21), and (22) appropriately, one may find all of the S-wave two-pseudoscalar partial widths of the scalar mesons, and, in some cases, close approximations to their total widths, by fitting the parameters r_2 , r_3 , and x to data. For $r_2 = 0.548i$, $r_3 = -0.258i$, $x_q = 3.034$, $x_K = -4.231$, and $x_s = 9.018$, the fit to existing states is achieved with considerable success.

Tbl. 3

Scalar meson	Mass (MeV)	Decay path	Theory (MeV)	Experiment (MeV)
$f_0(600)$	457 ± 13	$\rightarrow \pi\pi$	139.5	335 ± 67
$f_0(980)$	979 ± 6	$\rightarrow \pi\pi$	11.3	33.6 to 84.0
$f_0(1370)$	1342 ± 7	$\rightarrow \pi\pi$	45.0	52 to 130
		$\rightarrow \bar{K}K$	45.4	70 to 175
		$\rightarrow \eta\eta$	7.4	seen
		$\rightarrow P_i P_j$ (total)	97.8	129 to 321
$f_0(1500)$	1505 ± 7	$\rightarrow \pi\pi$	38.0	38.041 ± 2.507
		$\rightarrow \bar{K}K$	9.4	9.374 ± 1.090
		$\rightarrow \eta\eta$	5.6	5.559 ± 0.981
		$\rightarrow \eta\eta'$	----	2.071 ± 0.872
		$\rightarrow P_i P_j$ (total)	53.0	55.045 ± 8.225
$f_0(1710)$	1717 ± 6	$\rightarrow \pi\pi$	6.5	$\sim 6.54 \pm 3.04$
		$\rightarrow \bar{K}K$	77.1	$\sim 77.13 \pm 32.72$
		$\rightarrow \eta\eta$	0.4	$\sim 30.38 \pm 18.70$
		$\rightarrow \eta\eta'$	28.9	----
		$\rightarrow P_i P_j$ (total)	113.0	$<137 \pm 8$
$a_0(980)$	985 ± 6	$\rightarrow \eta\pi$	54.5	42.3 to 84.5
$a_0(1450)$	1475 ± 3	$\rightarrow \eta\pi$	179.9	$\sim 122.58 \pm 21.44$
		$\rightarrow \eta'\pi$	69.4	41.59 ± 19.01
		$\rightarrow \bar{K}K$	132.0	104.57 ± 27.33
		$\rightarrow P_i P_j$ (total)	381.4	265 ± 13
$K_0^*(800)$	797 ± 11	$\rightarrow K\pi$	200.5	618 ± 234
$K_0^*(1430)$	1412 ± 7	$\rightarrow K\pi$	243.9	275.72 ± 50.79
		$\rightarrow K\eta$	17.6	----
		$\rightarrow P_i P_j$ (total)	261.4	290 ± 21

Table 3 shows the theoretical scalar masses and partial widths as they would appear in nature, side by side with current experimental partial width values found in [7].

As table 3 indicates, the mixing model is rather successful, with all but four of the partial widths listed in table 4 falling acceptably close to or within experimental limits.

A more thorough investigation of pure state decays has also been pursued, and the fascinating results posted in this work. The finding of a resonance $X(1110)$ ($M = 1107 \pm 4$ MeV, $\Gamma = 111 \pm 8 \pm 15$ MeV) by Daftari *et. al.* [8], now in the PDG listings [1], and the presence of an unknown peak around 1630 MeV in E760 neutral data [9] indicate the possibility that pure or near-pure states may emerge in the scalar channel in certain reactions, such as $\bar{p}p$ annihilation. Using only the nonet isospin-0 mixing for

the pure $\bar{q}q$ scalar mesons, one finds that a theoretical state $f_0(1090)$ emerges with partial widths $\Gamma(\pi\pi) = 26.2$ MeV and $\Gamma(\bar{K}K) = 3.3$ MeV for a total width of $\Gamma = 29.5$ MeV, matching the mass of the reported resonance found by Daftari *et. al.* [8] in $\bar{p}n$ collisions. Perhaps this state is not so theoretical after all.

Also, the troubling width $\Gamma(f_0(600) \rightarrow \pi\pi)$ from this theory may be reconciled with experiment when the pure state decay of $f_0(\bar{q}^2 q^2)$ is considered. The $\bar{q}^2 q^2$ structure is dominant in $f_0(600)$, and the pure state decay of this state is considerably larger than the attained width here; one may assign a width closer to ~ 240 MeV considering that the $\bar{q}^2 q^2$ dominates $f_0(600)$, and may not survive long enough to enter other states such as $\bar{q}q$. This same rationale applied to the $K_0^*(800)$ shifts the width $\Gamma(K_0^*(800) \rightarrow K\pi)$ closer to ~ 400 MeV. Similarly, the troublingly small $f_0(980)$ total width may be reconciled by considering that its ratio $\gamma^2(\bar{K}K)/\gamma^2(\pi\pi) \approx 1$, allowing a large $\bar{K}K$ contribution due to its closeness to threshold.

Additionally, a pure glueball f_{gg} emerges with an interesting pattern of decays. Based on the parameter λ used earlier, the pure glueball decays appear to decay by ratios;

$$\gamma^2(\bar{K}K)/\gamma^2(\pi\pi) \approx 4\lambda/3 = 1.333 \tag{23}$$

In the case calculated here, the value of $\lambda = 1$ is easily obtained since $\Gamma(\pi\pi) = 18.6$ MeV and $\Gamma(\bar{K}K) = 21.8$ MeV. In E760 neutral data, a peak appears at about 1630 MeV which could be an f_{gg} shifted up by about 80 MeV due to constructive interference with $f_4(2050)$ and $f_6(2510)$ in the $3\pi^0$ background data. A sure way to tell if it is indeed an f_{gg} will be to measure the branching ratio $\Gamma(f_{gg} \rightarrow \eta\eta)/\Gamma(f_{gg} \rightarrow \pi\pi)$, which should be nearly zero for the pure-state scalar glueball, and may be deduced by comparing the integrated peak size in the $3\pi^0$ and $\pi^0\eta\eta$ backgrounds. This is opposed to the $f_0(1500)$ branching ratio value of 0.146 for the same process. If the comparison of the integrated peaks yields a branching ratio other than 0 or 0.146, and/or a mass above 1600 MeV, then the object is likely to be something other than a scalar meson or glueball.

The Latest Scalar Resonances

In the past two years, the experimental physics community has seen the proliferation of previously unknown scalar states in the 1 to 2 GeV range. These states can be explained if the radial excitation Regge trajectory for scalar mesons is based on the slope $\Delta M^2/\Delta n = 1.394 \text{ GeV}^2$; in this event, the states $f_0(1200 - 1600)$ ($M = 1480 \pm 150 \text{ MeV}$ or $1530 \pm 250 \text{ MeV}$, $\Gamma = 1030 \pm 170 \text{ MeV}$ or $560 \pm 40 \text{ MeV}$) [10] and $X(1810)$ ($M = 1812 \pm 26 \pm 18 \text{ MeV}$, $\Gamma = 105 \pm 20 \pm 28 \text{ MeV}$) [11] fall in line with the masses predicted for the radially-excited pure-state light scalar tetraquark and heavy scalar tetraquark respectively. Indeed, their decays all indicate an agreement with this scheme; $f_0(1200 - 1600)$ decays dominantly to $\pi\pi$ and $X(1810)$ decays into $\omega\phi$ (which is only possible for a heavy tetraquark). In the next year or so, there should be data to support that $X(1810)$ occurs in both $I = 0$ and $I = 1$ channels. As for the more familiar $K_0^*(1950)$, the assignment is still ambiguous, but leaning toward a radial excitation of the pure-state strange scalar meson. However, $f_0(1790)$ ($M = 1790 \pm 40 \text{ MeV}$, $\Gamma = 270 \pm 60 \text{ MeV}$) [12] does not appear to match any possible states that should occur below 2 GeV, and has been suggested to be a light scalar hybrid $\bar{q}qg$ [13] because of its OZI-violating appearance in $J/\psi \rightarrow \phi\pi\pi$.

Furthermore, an interesting and controversial experiment [17] has shown evidence of the suspected mix-on-mix-off behavior that would allow a pure glueball “echo” of sorts to be present in the E760 neutral data. The experiment, probing the σ resonance in high-energy pn collisions, found eight separate smaller-width resonances that combined to form a broad resonance-like sector. This is the behavior that I have hinted at... where mixing can be turned on or off, and with three mixings available one will find eight states from the Boolean algebra... acting like three switches and producing the observed nest of close-by states. It is this very behavior which I intend to capitalize on by further analysis of the E760 neutral data in search of a possible “pure glueball” scalar at about 1630 MeV.

Conclusion

In the grand scheme of things, the scalar mesons still represent a massive experimental challenge to the world. Recent attempts to explain all of the scalars in one framework, such as [14] and [15], have proven that standard theoretical phenomenologies do not explain the mass splittings or flavor content of the scalar mesons, as evidenced by their experimental masses or decays. As evidenced here in this work, however, the scalar mesons are still capable of being interpreted phenomenologically in a manner that manifests consistently good results, even with rather crude methods and calculations. It is hoped that this work will provide a new phenomenological tool for the prediction and assignment of scalar mesons as new data become available.

Acknowledgements

The author wishes to thank Dr. M. Abul Hasan for his continual support, guidance, and encouragement in high energy physics research pursuits, as well as Dr. Mark Strikman for his aid in the review process.

References

- [1] S. Eidelman *et. al.* (Particle Data Group), *Phys. Lett. B***592**, 1 (2004)
- [2] F. E. Close, An Introduction to Quarks and Partons, Academic Press: New York (1979), pgs. 88-89
- [3] K. Gottfried and V. Weisskopf, Concepts of Particle Physics, Oxford University Press: New York (1986), Vol. II pgs. 409-419
- [4] G. Bali *et. al.* (UKQCD), *Phys. Lett. B***389**, 378 (1993)
- [5] I. Caprini, C. Colangelo, and H. Leutwyler, hep-ph/0512364 (2005)
- [6] A. Kirk, hep-ph/0009168 (2000)
- [7] W. –M. Yao *et. al.* (Particle Data Group), *J. Phys. G***33**, 1 (2006)
- [8] I. Daftari *et. al.*, *Phys. Rev. Lett.* **58**, 859 (1987)
- [9] This data has come into my hands through research at Penn State University under the direction of Dr. M. A. Hasan, an emeritus member of the E760 Collaboration.
- [10] V. Anisovich *et. al.*, *Eur. Phys. J. A***16**, 229 (2003)
- [11] M. Ablikim *et. al.*(BES Collaboration), hep-ex/0602031 (2006)
- [12] M. Ablikim *et. al.*(BES Collaboration), *Phys. Lett. B***607**, 243 (2005)
- [13] X.G. He *et. al.*, hep-ph/0602075 (2006)
- [14] F. Giacosa, T. Gutsche, and A. Faessler, *Phys. Rev. C***71**, 025202 (2005)
- [15] T. Teshima, I. Kitamura, and N. Morisita, hep-ph/0501073 (2005)
- [16] J. Beringer *et. al.* (Particle Data Group), *Phys. Rev. D***86**, 010001 (2012)
- [17] Yu. A. Troyan *et. al.*, hep-ex/0811.4078 (2008)